Developmental Cell
Article

Flower Forms an Extracellular Code that Reveals the Fitness of a Cell to its Neighbors in *Drosophila*

Christa Rhiner,[1,2] Jesús M. López-Gay,[1,2] Davide Soldini,[1] Sergio Casas-Tinto,[1] Francisco A. Martín,[1] Luis Lombardía,[1] and Eduardo Moreno[1,*]
[1]Spanish National Cancer Centre (CNIO), Melchor Fernández Almagro 3, E-28029 Madrid, Spain
[2]These authors contributed equally to this work
*Correspondence: emoreno@cnio.es
DOI 10.1016/j.devcel.2010.05.010

SUMMARY

Cell competition promotes the elimination of weaker cells from a growing population. Here we investigate how cells of *Drosophila* wing imaginal discs distinguish "winners" from "losers" during cell competition. Using genomic and functional assays, we have identified several factors implicated in the process, including Flower (Fwe), a cell membrane protein conserved in multicellular animals. Our results suggest that Fwe is a component of the cell competition response that is required and sufficient to label cells as "winners" or "losers." In *Drosophila*, the *fwe* locus produces three isoforms, fwe^{ubi}, $fwe^{Lose\text{-}A}$, and $fwe^{Lose\text{-}B}$. Basal levels of fwe^{ubi} are constantly produced. During competition, the fwe^{Lose} isoforms are upregulated in prospective loser cells. Cell-cell comparison of relative fwe^{Lose} and fwe^{ubi} levels ultimately determines which cell undergoes apoptosis. This "extracellular code" may constitute an ancient mechanism to terminate competitive conflicts among cells.

INTRODUCTION

In metazoans, one mechanism by which suboptimal cells are culled is exemplified by the cellular interaction known as "cell competition" (reviewed in Milàn, 2002; Adachi-Yamada and O'Connor, 2004; Diaz and Moreno, 2005; Gallant, 2005). Cell competition was first described in *Drosophila* using mutations in ribosomal protein genes called *Minutes* (Morata and Ripoll, 1975; Simpson, 1979; Simpson and Morata, 1981). *Minute* homozygous flies are lethal, but heterozygotes are viable and normally sized, although it takes them longer to complete larval development due to lack of a fully active ribosomal machinery (Lambertsson, 1998; Marygold et al., 2007). However, when *Minute* heterozygous cells ($M^{/+}$) and wild-type (WT) cells are generated in the same wing disc, ($M^{/+}$) cells are no longer viable in the *Drosophila* wing (Moreno et al., 2002a). The fact that $M^{/+}$ cells are eliminated only when growing next to WT cells was the reason why this phenomenon was termed "cell competition" (Morata and Ripoll, 1975). Cell competition is now believed to be a method by which weaker cells are eliminated from a population in order to optimize tissue fitness (Moreno et al., 2002a).

Since the discovery of cell competition using *Minutes*, other genes have been linked to cell competition. Among them *dmyc*, the *Drosophila* homolog of the proto-oncogene *c-Myc* (Johnston et al., 1999), is best studied. Cells with higher levels of dMyc outcompete adjacent lower dMyc-expressing cells, which are eliminated by apoptosis (de la Cova et al., 2004; Moreno and Basler, 2004). dMyc can activate a variety of genes encoding components of protein synthesis pathways (Orian et al., 2003; Grewal et al., 2005) and therefore stimulate protein translation. Cells that overexpress dMyc but simultaneously harbor a mutation in a ribosomal protein gene in heterozygosis lose the ability to outcompete surrounding cells (Moreno and Basler, 2004), suggesting that the apposition of cells with unequal rates of protein synthesis is one of the triggers of cell competition.

Competitive interactions among cells are thought to be short range (Simpson and Morata, 1981) and are classically initiated by an insult, such as mutations in *Minute* or *dmyc* genes, which increases or decreases the fitness of a particular cell within the imaginal disc epithelium of *Drosophila*. This translates into imbalances in morphogen and survival factor signaling, because the cell with reduced fitness is less efficient at endocytosing several extracellular factors (Moreno et al., 2002a; Moreno and Basler, 2004; Diaz and Moreno, 2005). Through a yet-unknown mechanism, cells probably monitor the signaling levels of their neighbors and recognize distortions in the morphogen gradient (Adachi-Yamada et al., 1999; Adachi-Yamada and O'Connor, 2002). Winner cells are then thought to produce a killing signal of unknown identity (Senoo-Matsuda and Johnston, 2007). This ultimately leads to caspase activation in the "loser" cell (Moreno et al., 2002a), which in turn induces an engulfment response in the "winner" cell (Li and Baker, 2007). Because the expansion of winners occurs at the expense of losers, total cell numbers do not change and the normal pattern of the organ is preserved (Moreno and Basler, 2004). Therefore, it has been proposed that dmyc-induced supercompetition could play a role in early stages of cancer, when mutant cells overproliferate but still obey the overall organ size control mechanisms imposed by the genome (Moreno, 2008; Rhiner et al., 2009).

In this paper, we investigate how cells of *Drosophila* wing imaginal discs distinguish winners from losers during cell competition. We took a genomic approach and combined it with

functional assays in order to identify genes expressed early during the cell competition response. We found six markers upregulated early specifically in the loser cells: *CG9233, CG1084, CG4672, CG6151, CG2198,* and *CG3305*. Five of these genes encode for cell membrane proteins, suggesting that initial stages of cell competition rely heavily on cell-cell communication. We have further characterized *CG6151*. *CG6151* encodes for Flower, a cell membrane protein that is conserved in multicellular animals and proposed to be a Ca^{2+} channel in neurons (Yao et al., 2009). Our results suggest that differential expression of *CG6151* isoforms generate the scaffold and the extracellular epitopes required to mediate lose/win decisions during competitive interactions among cells of varying fitness.

RESULTS

A Genomic Approach to Study Cell Competition

We performed gene expression microarray analysis to identify novel molecular determinants and markers of the multistep process resulting in cell competition. It has been previously shown that cells expressing slightly higher levels of dMyc under the *tubulin* promoter (*tub > dmyc*) behave as supercompetitors and can outcompete neighboring WT cells, which in this setting perform as loser cells (de la Cova et al., 2004; Moreno and Basler, 2004). Therefore, a *tub > dmyc > Gal4* transgene was used that allowed the Flippase (Flp) recombinase-mediated generation of Gal4-expressing cells that are WT regarding *dmyc* expression and marked by including *UAS-lacz* or *UAS-GFP* reporters (Brand and Perrimon, 1993) (Figure 1A). Such GFP-positive WT cells were outcompeted in a spatial and temporal pattern characteristic for cell competition (Moreno and Basler, 2004). Control clones that expressed similar levels of Gal4 and GFP (*tub > cd2 > Gal4*), but were not surrounded by *tub > dmyc* cells (no competition), survived normally. Heat shock was optimized to maximize the amount of boundaries where GFP and non-GFP clones contact each other. mRNA was extracted from wing discs undergoing competition (*tub > dmyc > Gal4)* and control discs (*tub > cd2 > Gal4)* at different time points (0, 12, 24, and 48 hr) and the profiles were analyzed using BDGRC microarrays (see Figure S1 available online).

To exclude dMyc downstream targets, we eliminated all those genes whose expression was differentially regulated in discs with homogeneous high levels of dMyc (*tub > myc* discs). The genes we identified as differentially expressed during cell competition could be roughly divided into four categories: (1) upregulated early, (2) downregulated early, (3) upregulated late, and (4) downregulated late. Among the downregulated genes we found expected controls like Gal-4 and LacZ, because Gal-4 expressing LacZ/GFP-marked WT cells disappear when in competition. The set of upregulated late genes contained several proapoptotic factors. We were mainly interested in early upregulated genes that, according to the microarray data, were expressed as early as 12–24 hr after clone induction (ACI), because such genes could play an initiating role in the competition process.

To know whether those early upregulated genes were expressed in the loser or the winner cells, as well as to confirm our microarray data, mRNA fluorescence in situ hybridization (FISH) was performed in combination with antibody staining to visualize the GFP-positive WT cells in a *tub > dmyc* background (Figure 1A) or GFP-positive WT cells in a WT background (*tub > gal4*) (Figure 1C). Because GFP is typically lost during in situ hybridization, we developed a novel protocol to do FISH and antibody double staining that works efficiently (see Experimental Procedures). From the top ten early upregulated genes identified in the microarray (Figure S1), we could confirm at least six by in situ hybridization (Figure 1B): (1) *CG9233*, a zinc finger protein of unknown function (Celniker et al., 2002); (2) membrane GPI-anchored protein Contactin (*CG1084*) (Faivre-Sarrailh et al., 2004); (3) the transmembrane protein TMS1 (*CG4672*) (Celniker et al., 2002), a homolog of the serine incorporator family SERINC; (4) amalgam (*CG2198*), a cell membrane protein member of the immunoglobulin superfamily (Seeger et al., 1988); (5) the transmembrane protein Lamp (*CG3305*), found both cell membrane and lysosome-associated (Celniker et al., 2002); and (6) the transmembrane protein Flower (*CG6151*) (Yao et al., 2009). None of them had previously been described as a marker for cell competition. All six candidates were upregulated in the WT loser cells (Figure 1B) after induction of WT clones in a *tub > dmyc* background (Figure 1A), whereas no upregulation was detected in WT cells in a WT background (no competition) (Figures 1C and 1D).

Functional Analysis of Loser-Specific Genes by RNAi

To functionally analyze the role of those early loser-specific competition markers, we decided to knock-down the genes individually with *UAS-RNAi* constructs (Dietzl et al., 2007) in WT loser cells and quantify the number and size of remaining loser clones 72 hr ACI (Figure 2A). Again, transgenic flies of genotype *tub > dmyc > Gal4* allowed the Flp recombinase-mediated generation of Gal4-expressing cells that are WT regarding *dmyc* expression and marked by GFP. Clones of such GFP-positive WT cells were eliminated by *tub > dmyc* supercompetitors after 72 hr. When *UAS-RNAi* against the genes *CG1084* (*contactin*), *CG4672* (*TMS1*), and *CG2198* (*amalgam*) was specifically expressed in the loser cells, they were still eliminated similar to the controls where the *yellow* gene was targeted by RNAi or *UASlacz* was expressed instead (Figures 2A and 2B).

In contrast, when we tested *UAS-RNAi* against the genes *CG9233*, *CG3305* (*Lamp*), and *CG6151* (*Flower*) specifically in loser cells, they survived significantly better during cell competition. Seventy-two hours ACI, the rescue of WT clones using *UAS-RNAi* against *CG3305* (*Lamp*), *CG6151* (*Flower*), and *CG9233*, was comparable to the rescue obtained when apoptosis was blocked with the caspase inhibitor p35 (Hay et al., 1994), which is a known inhibitor of cell competition-induced apoptosis (Moreno et al., 2002a) (Figures 2A and 2B). Only expression of UASdMyc in the loser WT clones achieved a stronger rescue effect. The ultimate size of the surviving clones was comparable in all settings regardless whether RNAi was used (for example RNAi against *Flower*) or overexpression of dMyc, p35, or lacz (Figure 2C), but the number of remaining clones differed significantly 72 ACI (Figure 2B). All flies were previously examined at 24 hr to ensure that an equal amount of WT clones had been generated in all genotypes during heat shock (Figures S2A and S2B). Hereafter, we describe in more detail the function of *Flower* during cell competition. The role of the other genes will be discussed elsewhere.

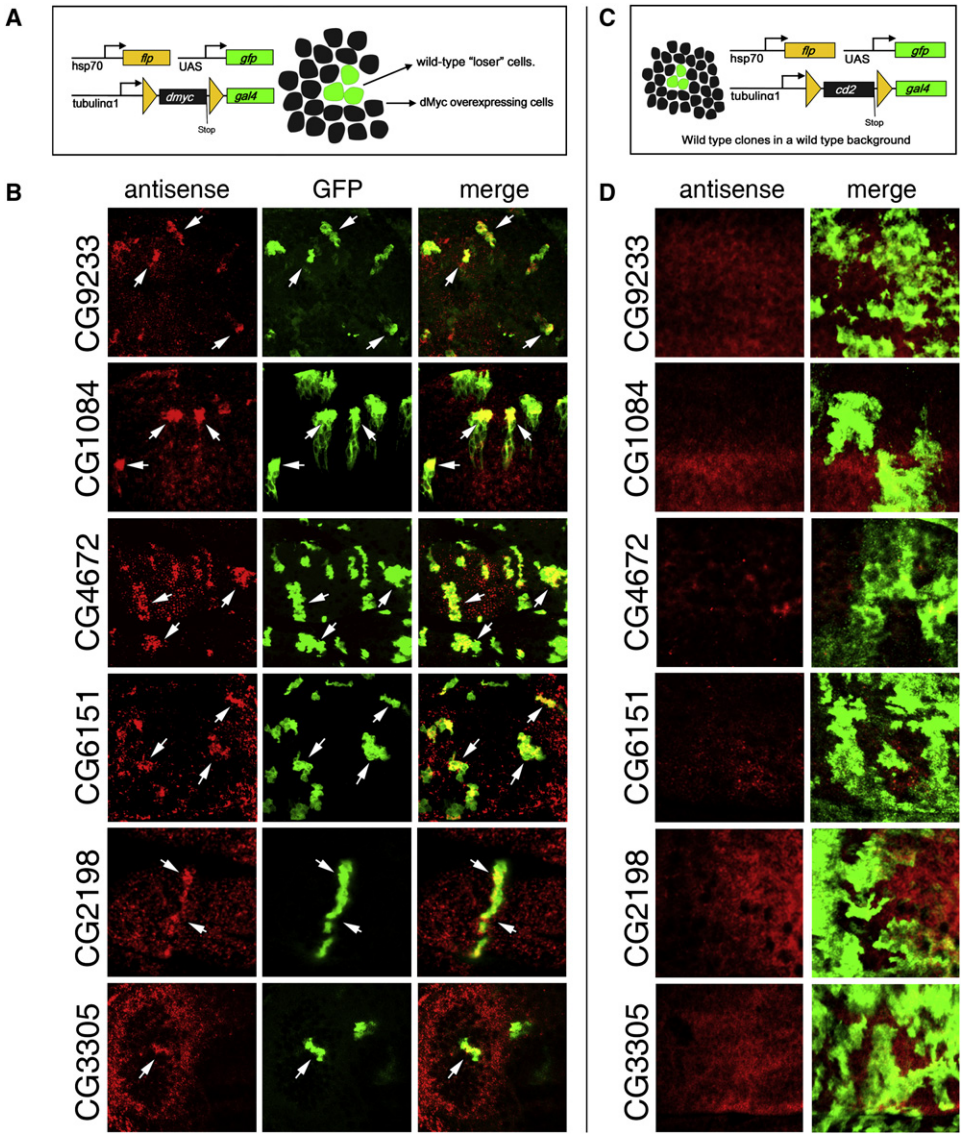

Figure 1. Molecular Markers Upregulated during dMyc-Promoted Cell Competition

(A) Flip-out technique used to generate GFP-marked wild-type (WT) cells in a dMyc-overexpressing background by combining three transgenes (*hs-Flp; tub > dmyc > Gal4/Cyo; UASgfp* flies). A short heat-shock (hs) activates the Flipase (Flp) enzyme in a random subset of cells leading to excision of a *dmyc* cassette flanked by FRT sites in the *tub > dmyc > Gal4* transgene. Upon removal of the *dmyc* cassette (including the stop codon), the *Gal4* gene is placed under the control of the *tubulin* promoter and subsequently activates *UAS-GFP* expression. This supercompetitor assay is depicted on the right at the cellular level. Clones of GFP-marked WT cells (green) are generated in a *tub > dmyc* background (black).

(B) In situ hybridization results (left panel, red) for six cell competition genes that showed an early-induced profile during cell competition in the microarray experiments. All depicted genes were found to be upregulated in the WT loser cell population (GFP-positive, middle panel, green) at 24–48 hr after clone induction (ACI). Merged images are shown in the right panel (arrows indicate colocalization).

(C) Control set-up based on the same Flip-out technique (see A) to generate GFP-marked WT cells in a WT background using *hs-Flp; tub > cd2 > Gal4/Cyo; UASgfp* flies. CD2 is membrane protein that does not interfere with the behavior of WT cells.

(D) In situ hybridization results (left panel, red) for the six markers in the absence of competition.

Flower (Fwe) Is a Conserved Metazoan-Specific Protein Located at the Cell Membrane

The *CG6151* locus encodes for Flower, a predicted protein with three or four transmembrane domains (Yao et al., 2009) and three isoforms of similar length that differ in their C-terminal part (Celniker et al., 2002) (Figure 3A). In order to verify the prediction of the three splice forms, we have fully sequenced the respective ESTs previously cloned by the BDGP. The protein sequence of Flower is conserved throughout evolution in all animals, from *Drosophila* to humans (Figure S2C). In silico predictions for the protein encoded by *flower (fwe)* suggested a conformation with an intracellular N-terminal part and an extracellularly exposed C terminus. We could confirm this for the three isoforms by transfecting S2 cells with various either C-terminally

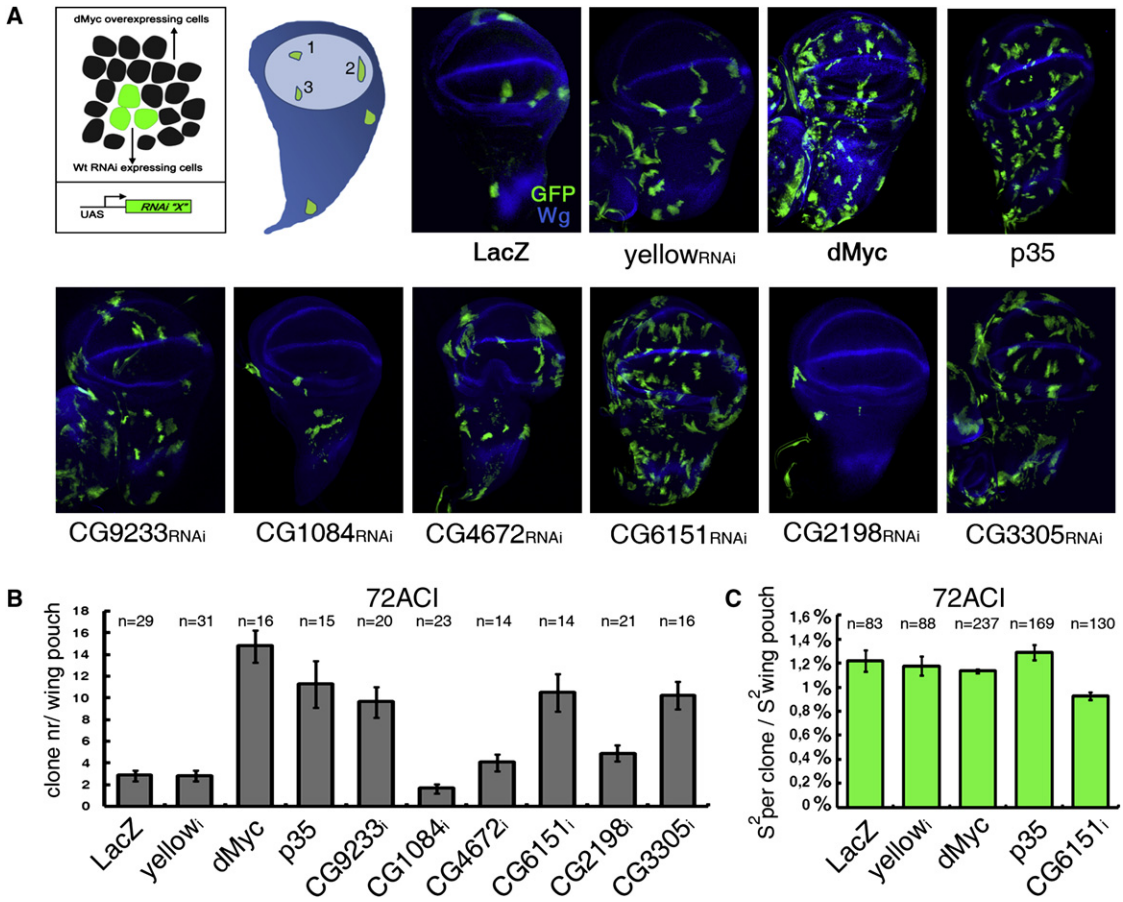

Figure 2. Functional RNAi Assay to Test Loser-Specific Genes

(A) Scheme depicting the activation of *UAS-RNAi* constructs against candidate genes specifically in the WT loser cells (green) that are confronted with dMyc-expressing supercompetitors (black). Imaginal wing discs of genotype *hs-Flp; tub > dmyc > Gal4/Cyo; UASgfp/UASRNAigene* were analyzed 72 hr ACI and remaining WT clones in the wing pouch (drawing, bright blue) were quantified. All discs were stained against Wingless (Wg) to delineate the wing pouch (blue). RNAi of the *yellow* gene and expression of *lacz* were used as negative controls, expression of the caspase inhibitor p35 and expression of dMyc are shown as a positive control for the assay.

(B) Quantification of remaining WT clones in the wing pouch 72 ACI ($n \geq 14$ discs, see graph). The graph depicts the average number of surviving clones per wing pouch for all genotypes.

(C) Graph showing the ratio of clone size/wing pouch area (%) for remaining WT clones at 72 ACI. $n \geq 83$ clones were quantified.

or N-terminally hemagglutinin (HA)-tagged constructs (Figures 3B–3E). S2 cells expressing Fwe isoforms with C-terminal HA tags could be detected with anti-HA antibodies in the absence of detergents (Figures 3B–3D), confirming that the C-terminal portion of the protein is exposed to the extracellular space. The same was observed when C-terminally HA-tagged proteins were expressed in the epithelial cells of the wing imaginal discs and stained with an in vivo protocol to detect extracellular epitopes (Strigini and Cohen, 2000; see Experimental Procedures) (Figures 3F and 3G). In contrast, HA tags located at the N terminus were only detected by anti-HA antibodies when transfected S2 cells were treated with detergents that destroy the integrity of the cell membrane and allow the antibodies to enter the intracellular space (not shown), but not in the absence of detergents (Figure 3E). Therefore, the protein products of *fwe* are most likely three-pass transmembrane proteins with an intracellular N-terminal part and an extracellular C terminus of variable sequence (Figure 3H). All three isoforms share the same scaffold but differ in their extracellularly exposed C-terminal epitopes (Figure 3H).

Three *fwe* Isoforms: *fwe*^{ubi}, *fwe*$^{Lose\text{-}A}$, and *fwe*$^{Lose\text{-}B}$

We next studied the expression patterns of the three isoforms of *fwe* in the imaginal tissues, both in the absence and presence of cell competition. To this end, we generated several isoform-specific RNA probes or antibodies because the probe that showed upregulation of *fwe* in the initial in situ recognized all three isoforms (*fwe* total, Figure 3A). First, we generated a monoclonal antibody that specifically recognizes the C terminus of one of the protein isoforms (Figures 3H–3L). This isoform was detected in all imaginal disc cells (Figures 3I–3L) and it localized to the apico-lateral membrane in wing imaginal disc (Figure 3N) and salivary gland cells (Figure 3O). Therefore, we named this isoform *fwe*^{ubi} because it is expressed ubiquitously in imaginal discs. Fwe^{ubi} stainings also colocalized with phalloidin, in accordance with membrane localization (Figure S3A). Activation of

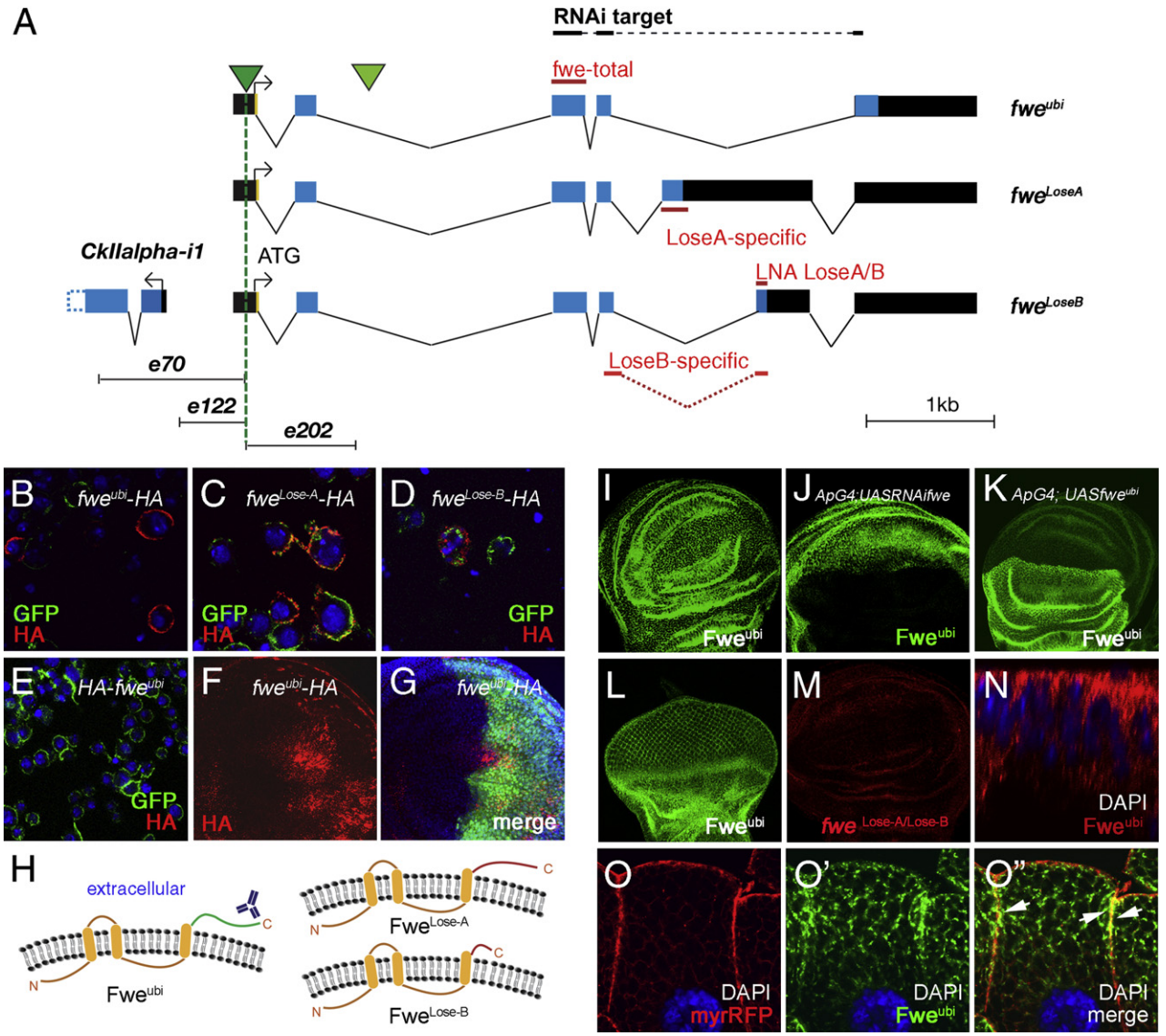

Figure 3. Flower (CG6151) Gene and Proteins

(A) Genomic structure of the *flower* (*CG6151*) locus. The three isoforms fwe^{ubi}, $fwe^{Lose\text{-}A}$, and $fwe^{Lose\text{-}B}$ are shown and the FISH mRNA probes used are marked at their hybridizing positions within the transcripts (red). The sequence targeted by the RNAi line is shown in black. The deletions in *fwe* mutants fwe^{e70}, fwe^{e122}, and fwe^{e202} are depicted with black bars at the bottom. Transposon insertions are shown with green triangles.

(B–E) S2 cells transfected with *UAS* plasmids containing (B) C-terminally HA-tagged fwe^{ubi} (C) C-terminally HA-tagged $fwe^{Lose\text{-}A}$ (D) C-terminally HA-tagged $fwe^{Lose\text{-}B}$ and (E) N-terminally HA-tagged fwe^{ubi}. *act-Gal4* (and *UASgfp)* plasmids were cotransfected to activate expression. Cells were stained for anti-HA (red) in the absence of detergent.

(F and G) Overexpression of C-terminally HA-tagged Fwe^{ubi} by *engrailed-Gal4* (*en-Gal4; UASfwe^{ubi}-HA*) in the posterior compartment (green) and stained for anti-HA (red) in the absence of detergent.

(H) The three isoforms, Fwe^{ubi}, $Fwe^{Lose\text{-}A}$, $Fwe^{Lose\text{-}B}$ differ only in their C-terminal extracellular epitopes.

(I) Endogenous expression of Fwe^{ubi} in the wing imaginal disc epithelium revealed with the Fwe^{ubi} antibody (green).

(J) Knockdown of *fwe* by RNAi targeted against the common region of all *fwe* isoforms, driven by *apterous-Gal4* (*Ap-Gal4; UASRNAi fwe*) in the dorsal compartment (anti-Fwe^{ubi}, green).

(K) Overexpression of Fwe using a *UAS-fwe^{ubi}* transgene, driven with *apterous-Gal4* in the dorsal compartment. Discs were stained with anti-Fwe^{ubi} (green).

(L) Endogenous expression of Fwe^{ubi} in the eye imaginal disc (Fwe^{ubi} antibody, green).

(M) Expression of fwe^{Lose} isoforms (red) is not detected in the absence of competition with none of the generated in situ hybridization probes (including the high-affinity LNA probe).

(N) Apico-lateral localization of Fwe^{ubi} (red) in the columnar epithelium of the wing imaginal disc. A cross section through a wing disc is shown. Nuclei are stained with DAPI (blue).

(O) Expression of Fwe^{ubi} in the big cells of the salivary glands. (O′) Fwe^{ubi} (green) accumulates at the apico-lateral membrane of the cells. The cell membrane is visualized by myristoylated RFP (red) (O). The merged image is shown on the right (O″). The Nucleus is marked with DAPI (blue).

UAS-fwe RNAi in the dorsal compartment, which targets all *fwe* isoforms, confirmed efficient downregulation of Fwe^{ubi} levels (Figures 3A and 3J). Similarly, overexpression of *UAS-fwe^{ubi}* driven by the dorsal *apterous-Gal4* promoter was easily detectable by the anti-Fwe^{ubi}-specific antibody (Figure 3K), whereas the same antibody did not cross-react with the two other forms when overexpressed in *act > y > gal4* clones or using the *apterous-Gal4* promoter (Figure S3B), confirming that it recognizes exclusively the Fwe^{ubi} form.

The two other splice forms were not expressed at detectable levels in imaginal discs in the absence of cell competition (Figure 3M), as revealed with a high-affinity LNA probe that specifically detects those two isoforms (Figures 3A and 3M). However, when WT cells were exposed to competition by *tub-dmyc* cells, these isoforms were specifically induced in the loser (WT) cells, as verified with the LNA probe recognizing both non-*fwe^{ubi}* forms or probes detecting only one of the two non-*fwe^{ubi}* isoforms (Figures 4A–4C). Because their expression appeared in loser cells, we termed them *fwe$^{Lose\text{-}A}$* and *fwe$^{Lose\text{-}B}$*, respectively. The *fwe^{Lose}* signal was typically detected throughout loser clones and not just at clonal boundaries (Figures 4A–4C) as it might be expected for short-range competitive interactions, suggesting that the triggered "Loser state" is somehow propagated within the clone.

The expression of *fwe Lose* isoforms was not induced in cells where apoptosis was triggered by other means than cell competition, e.g., targeted overexpression of *eiger* in the eye imaginal disc or clonal overexpression of activated *hemipterous*, the kinase activating *Drosophila* JNK (Adachi-Yamada et al., 1999) (Figures S4D and S4E). GMR-Gal4 driven expression of *UASeiger* in the eye leads to eye ablation as a consequence of massive JNK-dependent cell death (Moreno et al., 2002b). Coexpression of *UASeiger RNAi* or *UAShid RNAi* significantly rescued the eye ablation phenotype (Figures S4A and S4B; data not shown), whereas coactivation of *UASfwe RNAi* had no effect (Figure S4C), suggesting that *fwe* is a dedicated component of cell competition-induced apoptosis.

We next tested whether loser cells in other models of cell competition equally upregulate *fwe$^{Lose\text{-}A}$* and *fwe$^{Lose\text{-}B}$*, such as *Minutes (M$^{/+}$)* (Simpson and Morata, 1981), *thickveins* (*tkv*) (Burke and Basler, 1996) or *scribble* (Brumby and Richardson, 2003) mutant cells. Slowly proliferating *M$^{/+}$* cells in a WT background were generated with a translocation in the *Minute RpL19* gene and marked as described in Figure S4F. MARCM clones (Lee et al., 2000) in all three cell competition scenarios, *scribble −/−* cells, *tkv −/−* cells and *M$^{/+}$* cells in a WT background, induced *fwe^{Lose}* isoforms (Figures 4D–4F).

Overexpression of *fwe^{Lose}* in Clones Induces Apoptosis in S2 Cells and Imaginal Discs

To test whether *fwe$^{Lose\text{-}A}$* and *fwe$^{Lose\text{-}B}$* are sufficient to label cells as losers and trigger their elimination, we decided to activate *UAS-fwe$^{Lose\text{-}A}$* and *UAS-fwe$^{Lose\text{-}B}$* constructs in WT clones in the absence of (*dmyc*-induced) competition. Transgenic flies of genotype *act > yellow > Gal4*, allowed the Flp recombinase-mediated generation of Gal4-expressing clones to overexpress the respective UAS-constructs driven by the ubiquitous *actin* promoter (*act > Gal4; UASfwe*). Such cells were marked by the use of *UAS-GFP*, whereas surrounding WT cells expressed the *yellow* gene (*actin > yellow*), which does not induce competition. When *UAS-fwe$^{Lose\text{-}A}$* or *UAS-fwe$^{Lose\text{-}B}$* were specifically activated in GFP-marked WT cells surrounded by unmarked WT cells, the green Fwe^{Lose}-expressing cells tended to disappear from the tissue over a time course of 72 hr (Figures 5A–5C and 5G). Consistent with this, caspase was activated in *fwe$^{Lose\text{-}A}$* and *fwe$^{Lose\text{-}B}$*-expressing cells (Figure 5C, inset; Figures S5A and S5B). In general, *fwe$^{Lose\text{-}A}$* and *fwe$^{Lose\text{-}B}$* behaved indistinguishably in all experiments. In contrast, overexpression of Fwe^{ubi} did not interfere with the growth of such cells and large Fwe^{ubi}-expressing clones were observed 72 hr ACI (Figures 5D–5G), which were negative for Caspase 3 (data not shown). Cells expressing a construct encoding for a truncated *fwe* form without any C-terminal extracellular epitopes (*UASfwe^{delC}*) showed intermediate levels of apoptosis (Figures S5C–S5F).

To further corroborate the differential effects of *fwe^{ubi} versus fwe^{Lose}* expression in nonepithelial cells, we transfected macrophage-like *Drosophila* S2 cells with *ubi* or *-Lose* forms of *fwe* together with a *GFP* construct in a 20:1 ratio. Twenty-four hours after transfection, a 12 hr video was recorded. Cells transfected with *GFP* (Movie S1) or *fwe^{ubi}* (Movie S2) survived and did not show morphological changes. However, overexpression of *fwe^{Lose}* forms induced cell death. Interestingly, we observed a correlation between the length of interaction with nontransfected S2 cells and imminent cell death of the transfected cell. Analysis of the videos showed that apoptotic corpses first fragmented and then cellular debris were engulfed by surrounding nontransfected cells (Movies S3 and S4). *fwe^{Lose}*-expressing clones (*act > y < Gal4; UASfwe^{LoseB}*) generated in wing discs homozygously mutant for the *Drosophila* cell corpse engulfment receptor *draper* (Li and Baker, 2007), equally activated Caspase 3 at the clone border and underwent apoptosis (Figures S5G and S5H). Expression of *fwe^{delC}* was not sufficient to trigger apoptosis of S2 cells, in contrast to *fwe^{Lose}* forms (Movie S5).

From these experiments, we conclude that both *fwe$^{Lose\text{-}A}$* and *fwe$^{Lose\text{-}B}$* isoforms are sufficient to mark cells as losers in the presence of WT cells and trigger apoptosis in the absence of functional engulfment.

Neighboring Cells Participate in the Interpretation of Expressed *fwe^{Lose}* Isoforms

In order to distinguish if neighboring WT cells are required to detect and eliminate fwe^{Lose}-expressing cells or if fwe^{Lose} can trigger apoptosis cell autonomously, we performed a series of experiments where *fwe$^{Lose\text{-}A}$* or *fwe$^{Lose\text{-}B}$* was first expressed in large continuous clones and then ubiquitously in organs or the entire animal. Activation of *fwe^{Lose}* forms in large cell populations (polyclones), where most *fwe^{Lose}*-overexpressing cells lacked direct contact to WT cells, was achieved by applying long heat shocks to *act > y > Gal4* flies. Apoptosis in such *fwe^{Lose}*-overexpressing polyclones was diminished in the interior of the clone and a high proportion of apoptotic cells, revealed with anti-Caspase 3, was located specifically at the border of polyclones, where interaction with WT cells occurred (Figures 5H and 5I). Similarly, S2 cells cotransfected with any of the two *fwe^{Lose}* isoforms and *gfp*, but lacking direct cell-to-cell contact to nontransfected cells due to plating at low confluency did not undergo apoptosis (Movie S5). Finally, the importance of the presence of neighboring WT cells (that do not overexpress any *fwe^{Lose}*) to induce death of *fwe^{Lose}*-expressing cells is strikingly

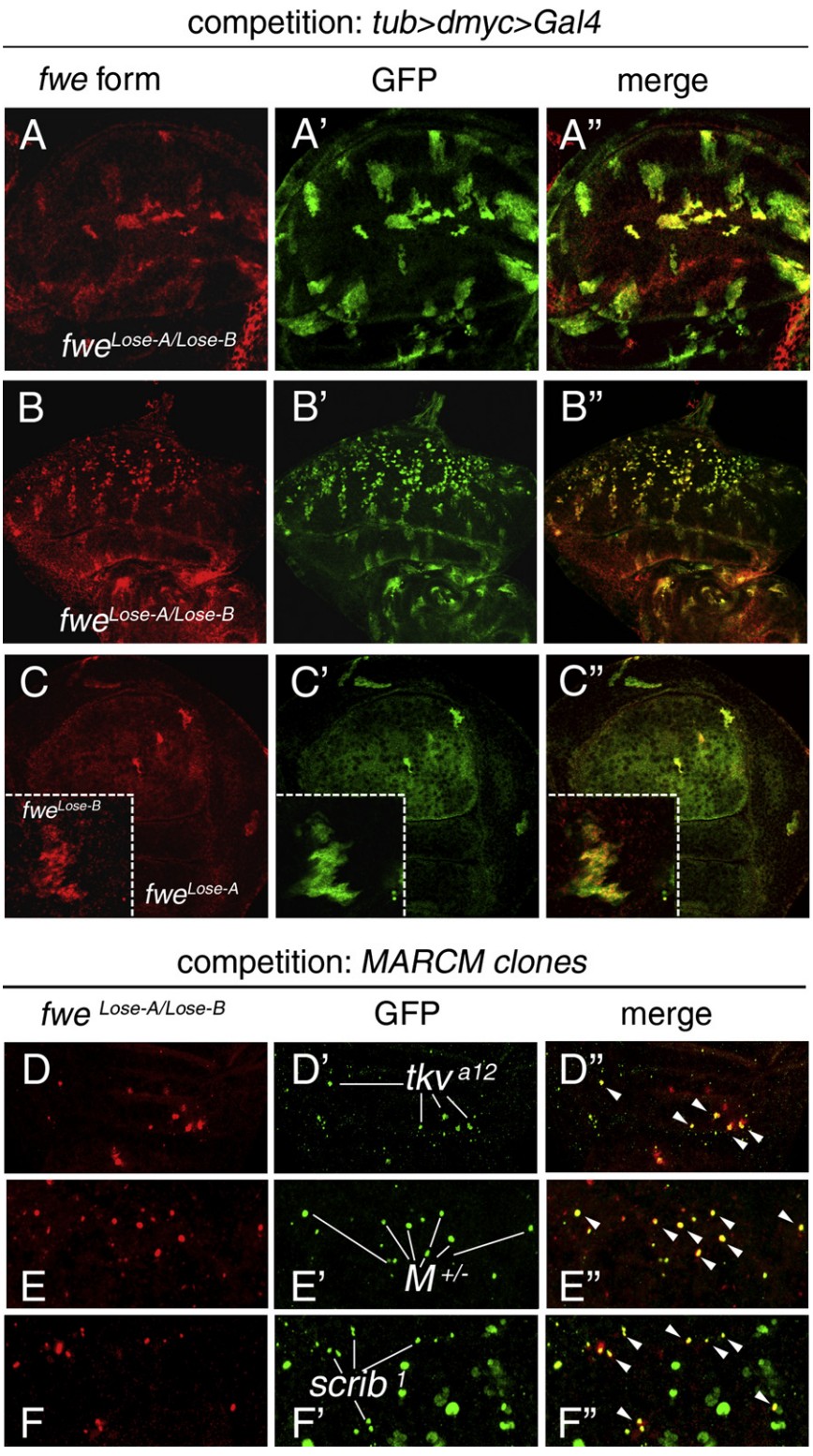

Figure 4. Upregulation of *fwe*^{Lose} Isoforms during Cell Competition

(A–F) Upregulation of *fwe*^{Lose} in *dmyc*-induced competition (A–C), in *tkv* mutant cells (D), *Minute*-triggered competition and in *scribble* mutant cells (F). (A and B) FISH using the LNA probe recognizing the common region of *fwe*$^{Lose-A}$ and *fwe*$^{Lose-B}$ (red). Competed WT clones marked with GFP (green) in the wing imaginal disc (A) and the eye imaginal disc (B), surrounded by *tub-dmyc* overexpressing cells (lack of green) (see Figure 1A). *fwe*$^{Lose-A}$ and/or *fwe*$^{Lose-B}$ are detected specifically in the loser cells (merge A and B). (C) FISH using mRNA probes recognizing *fwe*$^{Lose-A}$ (C, red) or *fwe*$^{Lose-B}$ (red, inset) in discs containing GFP-marked WT clones (green) in the wing imaginal disc, surrounded by *tub-dmyc* overexpressing cells (lack of green). (D–F) MARCM clones mutant for the Dpp receptor *tkv* (D), ribosomal genes (Minutes, *M*$^{/+}$ cells in a WT background) (E) (see Figure S4F) and *scribble* (F), which are marked by GFP, all upregulate *fwe*^{Lose} forms (red) under competition. Right panel shows colocalization of the in situ probe (red) with the MARCM clones (green). Flies of genotype *hs-Flp tub-Gal4 UAS-GFP; tkv*^{a12} *FRT40A / tub-Gal80 FRT40A* and *hs-Flp tub-Gal4 UAS-GFP; FRT82B scrib*^{1} */ FRT82B tub-Gal80* were used for (D) and (F), respectively.

illustrated in situations where all cells of the wing imaginal disc uniformly overexpress *UASfwe*^{Lose} under the *actin* promoter and no increase in apoptosis is observed (Figure 5J). Similarly, overexpression of Lose forms in an entire compartment does not affect disc size/morphology (Figure S3B). In fact, adult flies that ubiquitously overexpress homogeneous levels of the Lose isoforms activated by *act > Gal4; UASfwe*^{Lose} do not show any obvious defects (5K), which indicates that cells need to detect a relative difference in *fwe*^{Lose} levels in order to recognize and outcompete *fwe*^{Lose}-expressing cells.

Epistasis Analysis of *fwe*^{Lose} Expression

To further analyze how the *fwe*^{Lose} isoforms are specifically activated in the loser cells, we performed epistasis analyses. First, we checked if caspase activation is needed to trigger *fwe*$^{Lose-A}$ and *fwe*$^{Lose-B}$ induction as it is required, for example, for engulfment (Hoeppner et al., 2001). After blocking caspase activation specifically in loser cells with *UAS-p35* (Hay et al., 1994) (Figure 6A), *UAS-dIAP1* (the *Drosophila* inhibitor of apoptosis protein 1 (dIAP1) (Hay et al., 1995) (Figure 6B) or RNAi against the proapoptotic gene *hid* (Figure 6C) (Grether et al., 1995), *fwe*$^{Lose-A}$ and *fwe*$^{Lose-B}$ were still present at high levels in loser cells (Figures 6A–6C), despite the fact that these cells did not undergo apoptosis, proving that caspase activation is not required for *fwe*$^{Lose-A}$ and *fwe*$^{Lose-B}$ expression in loser cells.

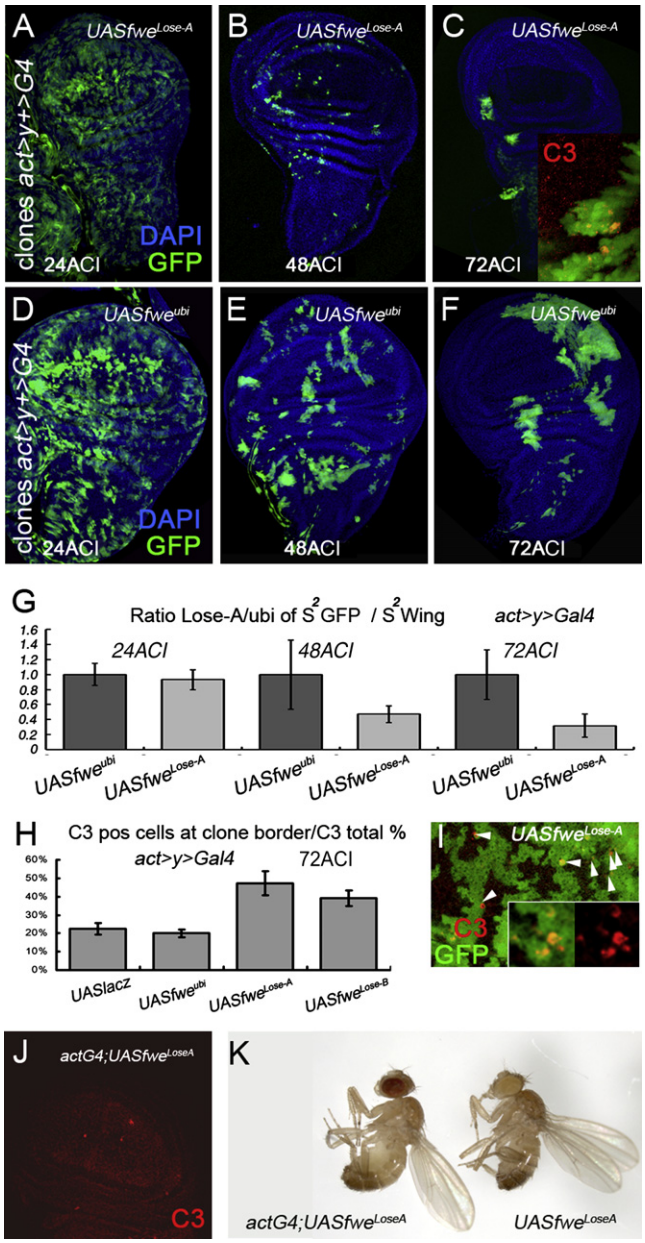

Figure 5. Overexpression of *fwe*^{Lose} in Clones Triggers Apoptosis

(A–F) GFP-marked cells overexpressing either *fwe*$^{Lose\text{-}A}$ (A–C) or *fwe*^{ubi} (D–F) with the *actin* promoter in a WT background (*act > yellow*) were generated by heat-shocking flies of genotype *hs-Flp; act > y > Gal4, UASgfp/UASgene*. Clones were analyzed at 24 hr (A and D), 48 hr (B and E), and 72 hr (C and F) ACI. Short heat-shocks of 8 min were used to induce few clones. (A–C) *Fwe*^{LoseA}-expressing clones at 48 ACI (B) and 72 ACI. Inset in (C) shows activated Caspase-3 (C3, red) induced inside GFP-marked clones overexpressing *fwe*$^{Lose\text{-}A}$ (green). (D–F) Fwe^{ubi}-overexpressing clones in a WT background 48 ACI (E) and 72 hr ACI. No induction of C3 is observed.

(G) Disappearance of Fwe^{LoseA}-expressing clones over time. Remaining GFP-positive area (S^2 GFP) was measured in relation to the total wing area (S^2 wing) at 24, 48, and 72 ACI. Clone size of Fwe^{Lose}-expressing cells was normalized to Fwe^{ubi}-expressing control clones. n = 18 discs were quantified.

(H) Graph depicting activated Caspase-3 (C3) positive cells located at clone borders as a percentage of total C3 positive cells. In all experiments quantified in H, longer heat shocks (15 min) were applied in order to generate polyclones overexpressing the different constructs. n ≥ 6 discs were quantified per genotype and a minimum of 140 apoptotic cells were analyzed.

(I) Apoptotic cells (revealed by anti-C3 staining) at clone borders of polyclones overexpressing *fwe*$^{Lose\text{-}A}$ marked by GFP (green).

(J) Disc overexpressing *fwe*$^{Lose\text{-}A}$ ubiquitously with the *actin* promoter (*actGal4; UASfwe*^{LoseA}) and stained by anti-activated Caspase-3 (red).

(K) *actin-Gal4* driven overexpression of *UASfwe*$^{Lose\text{-}A}$ allows normal growth and development (left). Flies that lack the *actin-Gal4* transgene to induce *UASfwe*$^{Lose\text{-}A}$ expression are shown as a control.

Next we tried to prevent *fwe*$^{Lose\text{-}A}$ and *fwe*$^{Lose\text{-}B}$ expression by interfering with an upstream event during cell competition such as imbalances in survival factor signaling. Because loser cells have been proposed to show a deficit in survival signaling (Moreno et al., 2002a; Moreno and Basler, 2004; Ziv et al., 2009), we overexpressed *UAS-dpp* (the *Drosophila* homolog of BMP2/4) in WT loser cells surrounded by supercompetitors. This reduced the levels of *fwe*$^{Lose\text{-}A}$ and *fwe*$^{Lose\text{-}B}$ activation as detected by FISH, but small WT clones surrounded by numerous supercompetitors and peripodial membrane cells (Figure 6D, arrowheads) still exhibited detectable *fwe*^{Lose} levels. Activating Rab 5 using a *UAS-rab5* construct, which stimulates endocytosis and rescues loser cells to a greater extent than Dpp overexpression (Moreno and Basler, 2004), strongly reduced levels of *fwe*^{Lose}, even in small clones (Figure 6E). This suggests that *fwe* functions downstream of events that affect the overall fitness of a cell leading to decreased endocytosis of survival factors. As a control, we performed RNAi in loser cells against the *fwe* sequence common to all isoforms (see Figure 3A), which efficiently suppressed the *fwe*^{LoseA} signal (Figure 6F).

Unlike the *fwe*^{Lose} isoforms, *fwe*^{ubi} was not upregulated in loser cells and rather seemed to be slightly downregulated. This was visible especially at late time points (96 hr ACI), probably due to Fwe^{ubi} protein perdurance (Figure 6G). In an alternative genetic set up, we created clones of WT cells growing in a slowly proliferating *M*$^{/+}$ background. Again, such M/+ cells showed upregulation of *fwe*^{Lose} and reduced levels of Fwe^{ubi}. The reduction of Fwe^{ubi} was subtle, but discernible in quantifications (Figures S6A–S6C). This raises the possibility that loser cells undergo a switch during cell competition leading to the upregulation of *fwe*$^{Lose\text{-}A}$ and *fwe*$^{Lose\text{-}B}$, probably at the expense of *fwe*^{ubi}.

Lack of *fwe*^{ubi} in Clones Triggers Apoptosis

In order to study the consequences of a decrease of Fwe^{ubi}, we generated *fwe* null mutants by inducing deletions via imprecise P-element excision. We obtained several deletions that affected the *fwe* locus, including two that remove the *fwe* promoter and 5′UTR (*fwe*^{e70} and *fwe*^{e122}) and one that eliminates the *fwe* 5′UTR and the first two exons (*fwe*^{e202}), including the start ATG in exon 1 (Figure 3A). All three deletions were lethal, probably due to early defects in nervous system formation (Figures S7A and S7B), and failed to complement although they removed different regions of the locus, proving that all of them are mutations in *fwe*. As expected from the type of lesion, *fwe*^{e202} clones did not show expression of *fwe*^{ubi} 96 hr ACI, confirming that it is a null mutation (Figure 7A). Because *fwe*^{ubi} is the only isoform detected in the wing imaginal cells in the absence of cell

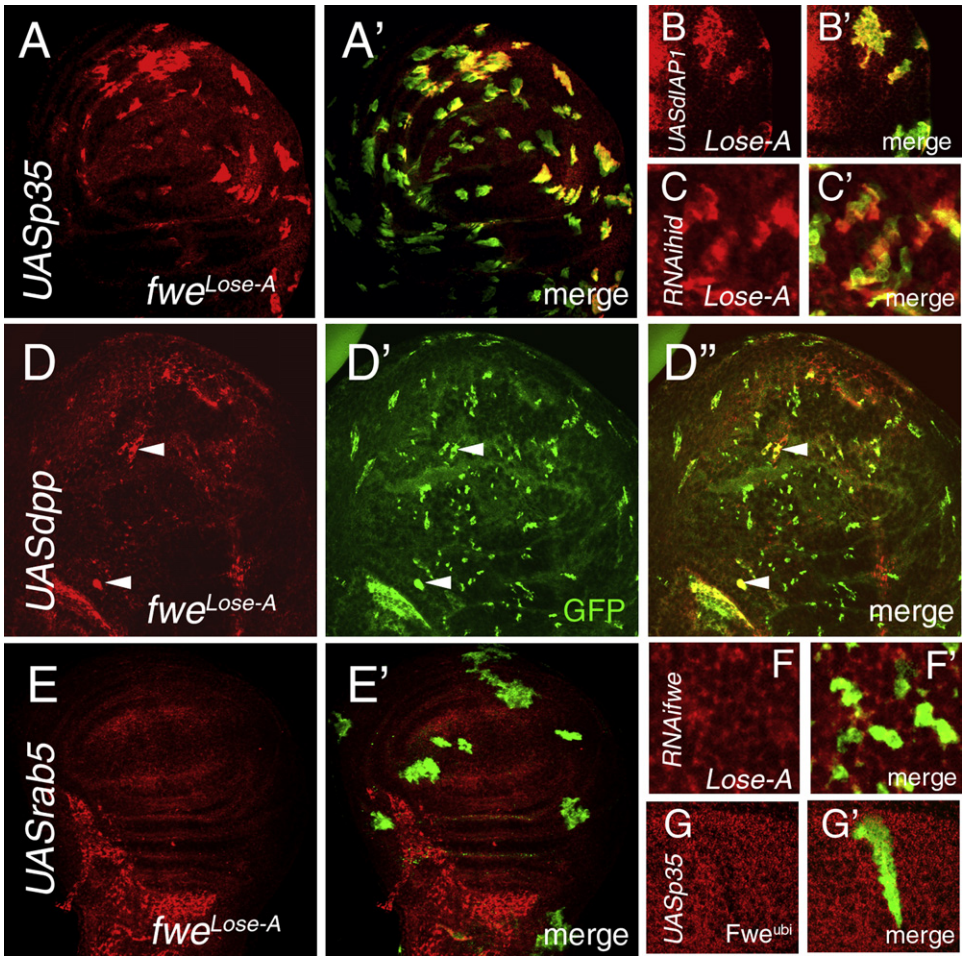

Figure 6. Epistasis Analysis of fwe^{Lose} Isoforms Expression

(A) In situ hybridization for *fwe^{LoseA}* (red) in *tub* > *Gal4* loser cells (green) (see Figure 1A) overexpressing *UASp35*.

(B) In situ signal for *fwe^{LoseA}* probe (red) in *tub* > *Gal4* loser cells (green) overexpressing dIAP1.

(C) *fwe^{LoseA}* in situ probe (red) in discs with *tub* > *Gal4* loser cells (green) expressing UAS RNAi against the pro-apoptotic gene *hid*.

(D) Overexpression of *UASdpp* in (tub > Gal4) loser cells (green). In situ hybridization for *fwe^{LoseA}* is shown in red. *fwe^{Lose}* signal is still detected in peripodial membrane cells (arrowheads).

(E) In situ hybridization for *fwe^{Lose}* forms in loser cells overexpressing UASRab5 (green). LNA-probe signal against the common region of *fwe^{Lose}* is shown in red.

(F) RNAi of the fwe locus in competed *tub* > *Gal4* loser cells (green) reduces the signal of *fwe^{LoseA}* (in situ probe, red). The same RNAi line also targets Fwe^{ubi} (Figure 3J).

(G) Fwe^{ubi} levels (red, Fwe^{ubi} antibody) 96 ACI in *tub* > *Gal4* loser cells (green, rescued by expression of UASp35).

competition, we could analyze its function using our null mutants. Most experiments were done with *fwe^{e202}*, but *fwe^{e122}* behaved identically. Clones of cells mutant for *fwe^{e202}* survived initially but were gradually eliminated from the wing imaginal discs (Figures 7B–7E) and were completely absent 120 hr ACI (Figure 7D). Consistent with this, *fwe^{e202}* mutant clones showed caspase activation 96 hr ACI (Figures 7B and 7C). The pattern of the *fwe$^{-/-}$* apoptotic cells was particularly striking, because C3-positive cells appeared in rings at the periphery of the clones (Figures 7B and 7C), indicating that *fwe$^{-/-}$* mutant cells in contact with Fwe^{ubi}-expressing cells were the first cells to be eliminated.

As expected from the expression pattern of the different *fwe* isoforms, only reintroducing Fwe^{ubi} with a UAS*fwe^{ubi}* transgene, but not expression of UAS Lose forms inside the *fwe$^{e202-/-}$* clones, using the MARCM system (Lee et al., 2000), could rescue cell death of *fwe* mutant cells revealed by an antibody that recognizes activated Caspase-3 (Figure 7F and data not shown), confirming that Fwe^{ubi} is the isoform required to restore cell survival. Lack of Fwe^{ubi} did not generally affect known survival transcription factors such as pMad (Tanimoto et al., 2000), dMyc (Johnston et al., 1999), or Vestigial (Halder et al., 1998), because *fwe$^{-/-}$* clones showed identical expression levels compared with neighboring WT cells (Figures S7C–S7E).

We next sought to determine if relative differences in Fwe^{ubi} expression are also involved in establishing win/lose decisions. To this end, we generated clones overexpressing the *UASfwe RNAi* used previously (Figure 2), which targets *fwe* exon-3 and 4 (Figure 3A), common to all *fwe* isoforms. However, this time we activated *fwe* RNAi in WT cells that are not suffering

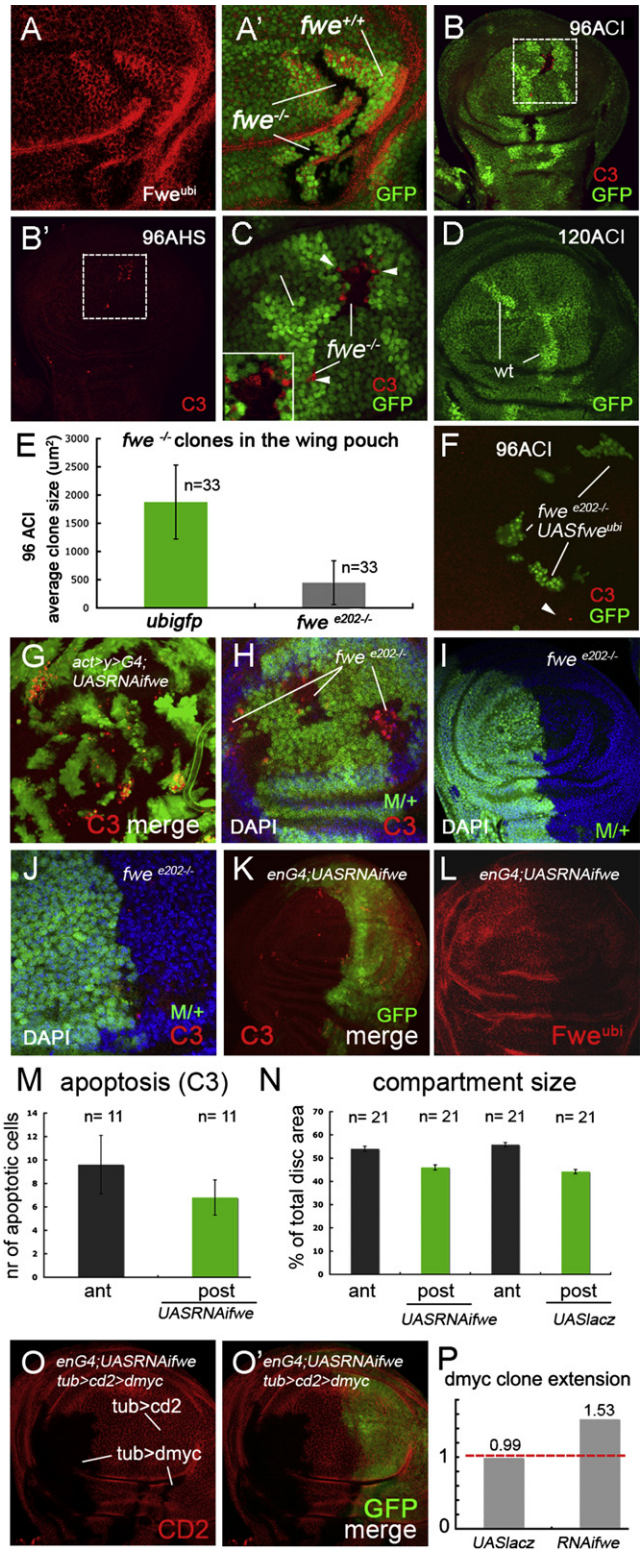

Figure 7. *fwe* Mediates Lose/Win Decisions during Cell Competition

(A) *fwe*$^{-/-}$ clones marked by lack of GFP (green, [A′]) do not show Fwe^{ubi} expression (Fwe^{ubi} antibody [red]) 96 hr ACI. Mitotic recombination clones were generated in *hs-Flp; fwe*^{e202} *FRT 80B/ ubigfp FRT80B* flies.

(B) Caspase activation ([B′], red) in *fwe*$^{-/-}$ cells (marked by lack of GFP, green) 96 hr ACI.

(C) Caspase positive fwe$^{-/-}$ cells (red, arrowheads) are contacting non mutant cells (GFP positive, green). See also inset.

(D) After 96–120 hr, most of the *fwe*$^{-/-}$ clones have been eliminated and only the twin spots are visible (two copies of GFP, brighter green).

(E) Quantification of clone size 72–96 hr ACI for *fwe*$^{-/-}$ and respective twin spots in the wing pouch.

(F) Overexpression of *fwe*^{ubi} using a UAS construct inside the *fwe*$^{-/-}$ cells (marked with GFP using the MARCM system, green). Caspase activation (red, arrowhead). Mitotic recombination clones were generated in *hs-Flp, tub-Gal4, UAS-gfp; UAS-fwe*$^{ubi/+}$*; fwe*^{e202} *FRT 80B/ tub-Gal80 FRT80B* flies.

(G) RNAi of the *fwe* locus in clones (*act > y > Gal4; UASRNAi fwe*) induces activated Caspase-3 (red) in GFP-marked clones (green) surrounded by WT cells 96 hr ACI.

(H) The +/+ cells mutant for *fwe* (black) located next to Minute cells (*M*′$^{/+}$, green) activate Caspase 3 (red). Mitotic recombination clones were generated in *hs-Flp; fwe*^{e202} *FRT 80B/ubigfp, RpS17- FRT80B* flies. Nuclei are stained with DAPI.

(I) Wing disc with anterior compartment formed by Minute cells (*M*′$^{/+}$, green) and posterior compartment composed entirely of *fwe*$^{-/-}$ cells (black) using the Minute technique (see Supplemental Experimental Procedures). Nuclei are stained with DAPI to visualize the disc morphology.

(J) Inset of the same disc in (I) stained with anti-Caspase 3 (red).

(K and L) Disc where RNAi against *fwe* is driven by *engrailed-Gal4* in the entire posterior compartment (K, green). Staining for activated Caspase-3 (red). (L) shows downregulation of Fwe^{ubi} levels (red in L).

(M) Graph depicting the number of apoptotic cells in anterior versus posterior compartment. N = 11 wing discs were quantified.

(N) Compartment and wing disc size of discs where *UASfwe* RNAi (left) or UAS-lacz (right) was activated in the posterior compartment using the *engrailed-Gal4* driver, n = 21 wing discs per genotype.

(O) dMyc-overexpressing supercompetitors (black, *tub > dmyc*) were induced in a background of CD2-expressing WT cells (red, *tub > cd2*) using *hs-Flp EnGal4 UASgfp/Cyo; tub > cd2 > dmyc/ UASRNAifwe* flies. Discs were analyzed 120 hr ACI. (O′) RNAi effect of *fwe* in the posterior compartment (green).

(P) Graph depicting the relative growth ratio (% area occupied by *dmyc* supercompetitors) in the anterior versus posterior compartment in the presence of *fwe RNAi* or with control expression of *UASlacz* on the posterior side. N > 60 *tub > dmyc* clones were analyzed for anterior compartments and n > 40 *tub > dmyc* clones on the posterior side. The red bar marks a growth ratio of 1, obtained when supercompetitor clones expand at the same rate in both compartments.

from cell competition (*act > yellow > Gal4; UASfwe RNAi*) and therefore only express the *fwe*^{ubi} isoform. After Flippase induction, such cells were marked by *UAS-GFP* and overexpressed the RNAi against *fwe (act > Gal4;UASfweRNAi)*. Clones of cells with downregulated *fwe*^{ubi} levels activated Caspase 3 and tended to die 96 hr after clone induction when surrounded by cells with WT levels of *fwe*^{ubi} (Figure 7G).

Death of Cells Lacking *fwe*^{ubi} Is Not Due to Growth Defects

Because death of *fwe* mutant and *fwe* RNAied cells could be due to cell autonomous growth defects, we next devised an experiment where *fwe* is removed in cells with a proliferative advantage because they are facing *Minute* (*M*′$^{/+}$) cells (Figures 7H–7J; see Experimental Procedures).

First, we carefully proved that $^{+/+}$*; fwe*$^{-/-}$ cells have indeed a proliferative advantage over *M*′$^{/+}$ cells. In order to test this we took advantage of the fact that such cells can form full posterior compartments homozygously mutant for *fwe* (Figures 7I and 7J). We found that those compartments reach their final size before the neighboring anterior compartment. For example, when

dissected early in development (Martín and Morata, 2006), the size ratio posterior versus anterior compartment" (P/A ratio) in *fwe/M* compartments is 0.73 in contrast to the maximum P/A ratio of 0.65 in a WT/WT disc, and similar to previous results of 0.7 for a WT/M disc P/A ratio, (Martín and Morata, 2006). This confirms that *Minute*$^{+/+}$*; fwe*$^{-/-}$ cells indeed have a growth advantage (Figures 7I and 7J).

Despite this growth advantage, the *Minute*$^{+/+}$*; fwe*$^{-/-}$ cells are forced to activate Caspase-3 (25 out of 31 clones showed massive signs of apoptosis) when coexisting in the same compartment with *M*$^{/+}$ cells expressing *fwe*^{ubi} (Figure 7H), but not when all the cells of the compartment lack *fwe* (Figures 7I and 7J). The death of *fwe*$^{-/-}$ cells is caused solely by the presence of neighboring Fwe-expressing cells, independent of differential growth rates.

Consistent with the results shown in Figures 7I and 7J, homogeneous knockdown of *fwe* levels in a whole compartment using the *UASfwe RNAi* used previously and the *engrailed-Gal4* driver (Figures 7K and 7L) did not induce increased apoptosis as revealed with anti-Caspase 3 antibody (Figures 7K and 7M) nor affect compartment growth (Figure 7N), despite strongly reduced levels of Fwe^{ubi} in the posterior compartment (Figure 7L).

This illustrates that lack of Fwe^{ubi} does only induce apoptosis when *fwe*$^{-/-}$ cells interact with neighbors expressing WT levels of Fwe^{ubi}, independent of their differential growth rates.

Fwe Specifically Regulates Cell Competition-Mediated Growth and Not Normal Growth

Our initial epistasis experiment showed that knockdown of all three *fwe* forms exclusively in loser cells can inhibit/delay competitive interactions (Figure 2). We next studied what happens to cell competition if *fwe* is knocked down in a whole compartment. To this end, we monitored the spread of *tub > dmyc* supercompetitors in a WT background (*tub > cd2*), in discs where RNAi of *fwe* was exclusively activated in the posterior compartment (*hs-flp; en-Gal4, UAS-gfp*$^{/+}$*; UASfwe RNAi/ tub > cd2 > dmyc*) (Figures 7O and 7P). *tub > dmyc* supercompetitors grew equally in both compartments when *UAS-lacz* was expressed on the posterior side as a control (clone size in A/clone size in P ratio = 0.99) (Figure 7P) as previously reported (Moreno and Basler, 2004). In contrast, RNAi of *fwe* significantly reduced the expansion of dMyc-overexpressing clones on the posterior side (clone size in A/clone size in P ratio = 1.53 (Figures 7O and 7P), without affecting overall growth of the posterior compartment (Figures 7N and 7O). This epistasis experiment shows that *fwe* reduction of function in both winner and loser cells exclusively affects cell competition mediated growth, whereas it does not interfere with normal tissue growth.

DISCUSSION

Here we have explored how cells of *Drosophila* wing imaginal discs distinguish winners from losers during cell competition. Five out of six genes identified in our screen for early competition markers were membrane proteins pointing to an important role of cell-to-cell communication during the initial phase of cell competition. Our results suggest that the membrane protein Fwe (CG6151) is a dedicated component of the cell competition response that is required and sufficient to label cells as "winners" or "losers."

Fwe mediates win/lose decision by means of three differentially expressed isoforms, *fwe*^{ubi}, *fwe*^{LoseA}, and *fwe*^{LoseB}. Cells are identified as losers when relative differences of *fwe*^{ubi} or *fwe*^{Lose} levels are detected (Figure 8). This system bears the advantage that cells are able to survive general stress conditions that uniformly affect the entire population within a compartment. We propose that, in outcompeted cells, the *fwe* transcript is alternatively spliced and *fwe*^{Lose} isoforms are induced at the expense of *fwe*^{ubi}. Probably both, the downregulation of *fwe*^{ubi}, as well as the upregulation of *fwe*^{Lose} contribute to establish the lose/win decision. We do not yet know how the alternative splicing is regulated. The simplest possibility is that when cells competing unsuccessfully for extracellular resources are deprived of survival factors (Diaz and Moreno, 2005), they are also depleted from some crucial splicing factors and default splicing will result in the formation of the normally repressed Lose forms. The observation that *fwe*^{Lose} upregulation was usually detected throughout the entire loser clone and not just at clone borders could be the consequence of a mechanism that propagates the "loser" state in outcompeted clones. We consider two hypotheses as likely: a cell-to-cell signal that efficiently transmits the "Lose verdict" among outcompeted cells. Alternatively, border cells may transiently increase their uptake of survival factors such as Dpp, for example by generating cytoneme-like extensions (Hsiung et al., 2005), which would further deplete survival factors in the interior of the loser clone.

What Type of Gene Is *fwe*?

fwe shares certain features with proapoptotic or growth promoting genes with respect to cell competition, but overall it behaves differently and seems to stand in a class of its own.

Genes mediating apoptosis (*hid, reaper*) show a similar behavior to *fwe*^{Lose} in certain aspects, in that they are triggered in loser cells and their elimination inhibits cell competition-induced apoptosis. Likewise, Fwe^{Lose} can trigger cell death in clones in the absence of cell competition. However, such proapoptotic factors induce apoptosis when overexpressed ubiquitously, whereas overexpression of *fwe*^{Lose} (or lack of *fwe*^{ubi}) throughout the wing imaginal disc or in the entire fly does not interfere with cell viability nor organ size. This context-dependence implicates that *fwe* does not work as a simple killing signal or some sort of toxic protein acting cell autonomously.

Fwe also shares features with genes known to affect normal tissue growth like *Minutes (M*$^{/+}$*)* or *dmyc* such as cell-nonautonomous effects on survival in a heterotypic background. Homozygously mutant *fwe* cells show normal survival when all cells of one compartment are of the same genotype, but they are forced to undergo apoptosis when surrounded by wt cells, a hallmark of cell competition. However, this death does not depend on growth differences: (a) *fwe*$^{-/-}$ cells are forced to activate caspase-3 in the presence of *Minute* cells, which have a lower proliferation rate, but do express *fwe*^{ubi}; and (b) removal or downregulation of *fwe* throughout a compartment specifically inhibits cell competition without affecting the growth rate of the whole compartment.

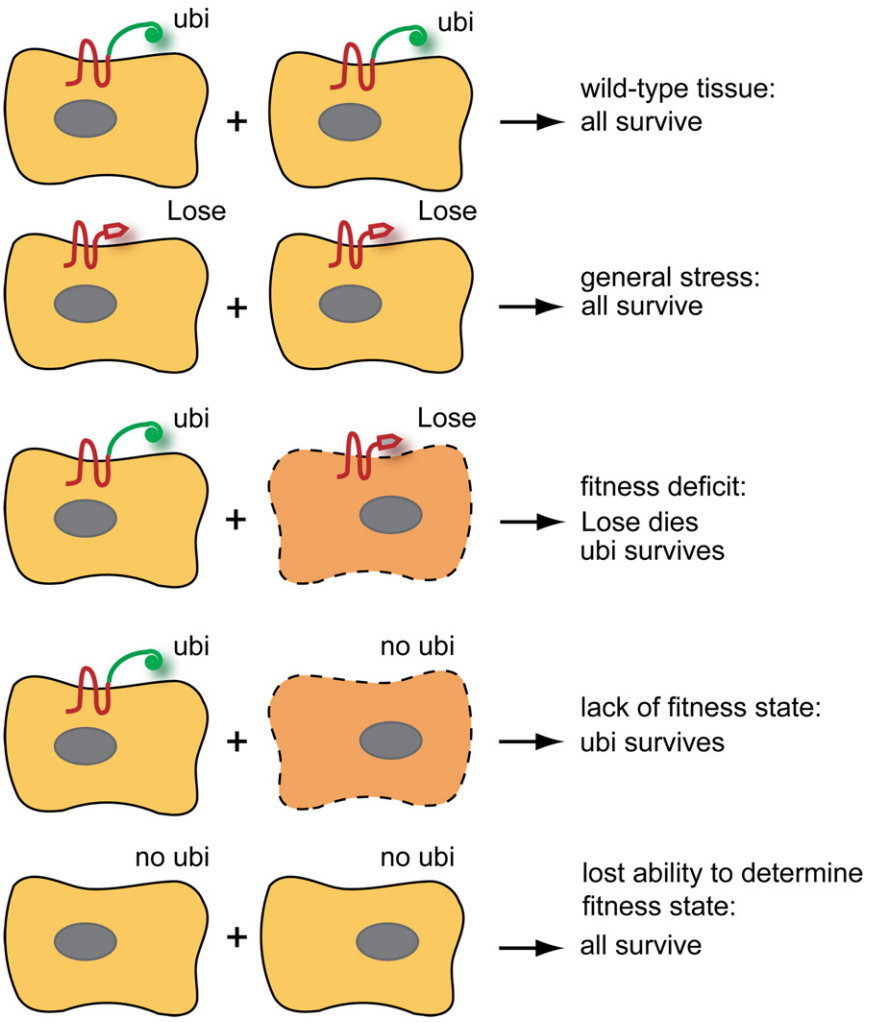

Figure 8. Model of Fwe-Dependent Cell-Cell Communication Mediating Lose/Win Decisions during Cell Competition

In a healthy tissue, cells constantly produce high levels of Fwe^{ubi} (green sprout), which signal intact cellular fitness (Figures 3I and 3L). Uniform upregulation of Fwe^{Lose} forms (red rocket), does not trigger cell competition-induced cell death (no relative differences present) (see Figures 6J and 6K). However, an insult leading to a fitness deficit in a single cell or a small group of cells induces the expression and exposure of Fwe^{Lose} (red rocket) (Figure 4). Such suboptimal cells, labeled with Fwe^{Lose} epitopes, are recognized by surrounding WT cells and forced to undergo apoptosis (Figures 5A–5H; Figures S5A and S5B and Movise S1–S5). Cell competition is also initiated if a cell surrounded by Fwe^{ubi}-expressing WT cells fails to express Fwe^{ubi} or produces only low levels (Figures 7A–7G). If *fwe* is lost in an entire tissue (Figures 7I and 7J), cell competition cannot occur and suboptimal cells may accumulate.

It has been proposed that Fwe is a calcium channel (Yao et al., 2009). However, during cell competition we observe antagonistic functions for the different isoforms, unlike in synaptic vesicles where the two isoforms that we call here Ubi and Lose A seem to be functionally equivalent (Yao et al., 2009).

Finally, our data show that fwe^{Lose} is not just an "eat me signal" because *fwe Lose* forms are able to trigger Caspase-3 activation and cause cell death before and in the absence of functional engulfment (; Figures S5G and S5H).

Extracellular Epitopes Reveal Cell Fitness: The Flower Code

We propose that within a multicellular organ cells are constantly tagged by extracellularly exposed Fwe epitopes that function as a code. This extracellular code is composed by different Fwe isoforms and allows comparison of relative fitness. During cell competition in *Drosophila,* the *fwe* isoforms work as a simple ternary code (fwe^{ubi}, $fwe^{Lose\text{-}A}$, and $fwe^{Lose\text{-}B}$) with a binary output, because fwe^{ubi} is translated as "intact cellular fitness" whereas $fwe^{Lose\text{-}A}$ and $fwe^{Lose\text{-}B}$ are redundant and lead to cell elimination (Figure 8). The experiments with the C-terminally truncated Fwe form suggest that the presence of the Lose epitopes aid in the labeling of cells as losers, although the lack of the ubi tail may also help in their elimination.

We expect other molecules to interact with Fwe, which are able to interpret the thresholds or read the extracellular epitopes displayed by the Fwe isoforms. It is likely that the signal recognized by neighboring cells includes not only the variable C-terminal epitopes, but also the constant extracellular loop because its sequence is conserved from flies to humans.

The "code" composed by the Fwe isoforms may have biomedical implications beyond cell competition because imbalances in cell fitness appear during aging, cancer formation, and metastasis.

EXPERIMENTAL PROCEDURES

Microarray

For the microarrays, marked WT cells were generated in a dMyc-overexpressing background with the *tub > dmyc > Gal4* transgene as described in Moreno and Basler (2004). For control clones, the *tub > cd2 > dmyc* transgene was used instead. Heat shock was optimized to maximize the amount of boundaries where GFP and non-GFP clones contact each other, and mRNA was extracted with TRIzol reagent (Invitrogen) and RNeasy (Quiagen) from both genetic setups at 0, 12, 24, and 48 hr and the profiles were analyzed using BDGRC microarrays.

Immunohistochemistry

Primary antibodies used were anti-GFP (rabbit, 1:200; Abcam; and 1:300; Invitrogen), anti-β Gal (rabbit, 1:1000, Cappel), anti-C3 antibody (rabbit, 1:300; Cell Signaling), anti-repo (mouse, 1:50; Developmental Hybridoma Bank), anti-Wg (mouse, 1:50; Developmental Hybridoma Bank), anti-HA (rat, 1:500 in imaginal discs, 1:100 in cells; Roche), anti-Vestigial (rabbit, 1:100, a gift of

Sean Carroll; and 1:50, guinea pig, a gift of Gines Morata), anti-Brinker (rabbit, 1:300), anti-dMyc (guinea pig, 1:300), and anti-pMad (rabbit, 1:300) (all three gifts of Gines Morata). Phalloidin Alexa-488 was applied 1:100 (Molecular Probes).

To generate specific antibodies against the Fwe^{ubi} isoform, a synthetic peptide with the C-terminal sequence (NNAQPFSFTGAVGTDSNV) was used to immunize mice and generate monoclonal antibodies. Anti-Fwe^{ubi} antibodies were used 1:30. Stainings were performed using standard procedures except for the staining of Figure 3F, where the protocol described by Strigini and Cohen, (2000) was used. Embryos were dechorionated in 30% bleach and fixed in 4% PFA according to standard procedures. Images were taken in a SP2 or SP5 Zeiss confocal microscope and analyzed with Adobe Photoshop CS2 and ImageJ 1.41.

mRNA FISH and GFP Double Staining

Larvae were dissected in sterile-filtered phosphate-buffered saline (PBS) on ice, fixed for 20 min in filtered 4% PFA/0.4% PBS-Triton-X (PBT) on ice and washed in PBT (0.4%). Then, larvae were incubated for 10 min in hybridization buffer (HB)/PBT (1:1) for 10 min, followed by blocking in HB for 1–2 hr. 500–800 ng mRNA probe was diluted in HB and hybridized for 48 hr at 56°C. The LNA-probe against *fwe*$^{Lose\text{-}A/Lose\text{-}B}$ (Exiqon) was used at a concentration of 2.5 pM with a hybridization time of 24 hr at 56°C.

Larvae were then washed twice in HB (at 56°) for 10 min followed by rehydration in prewarmed (56°C) HB:PBT (3:1, 1:1, 1:3) at room temperature for 30 min each. After rehydration, samples were washed in PBT and blocked with PBT-BSA (1%). Antibodies used to detect DIG-labeled probes and loser cells were anti-DIG (mouse, 1: 750) (Jackson) and anti-GFP (rabbit, 1:200) (Abcam), respectively. The Dig signal was amplified with biotinylated anti-mouse (1:200) (Jackson) followed by Tyramide amplification (Invitrogen).

Primers used to generate specific CG6151 probes by in vitro transcription (Roche) were:

CG6151:ATTTAGGTGACACTATAGAAGAGTTCGGCCTGTGGAATGTG/TAATACGACTCACTATAGGGAGACACGGAAGTACAAGGGCT

Lose-A: ATTTAGGTGACACTATAGAAGAGGCTTCTCGAGAGGACATGG/TAATACGACTCACTATAGGGAGAGGCGCCAGACATCGG

*Lose-B:*ATTTAGGTGACACTATAGAAGAGGCCATTCCGCCCATTAT/TAATACGACTCACTATAGGGAGAATAGGTTCCGGTTCCTCT

LNA-probe (recognizing both Lose isoforms): CATTCGGTTAGCTTTCAAATATAGT.

fwe Mutants

Deletions in the *fwe* locus were obtained by imprecise excision of transposon P(EPgy2) in the strain *CG6151*^{EY08496} (Bloomington). Transposon jumping was induced by crossing flies to a transposase source (delta 2-3). Recovered transposon jumps were balanced and DNA of > 250 established stocks screened for deletions in *fwe*. Three different deletions were recovered: *fwe*^{e70}, *fwe*^{e122}, and *fwe*^{e202}. *E202* is a clean deletion in the *fwe* locus of 957 bps, which removes exon 1 (including the ATG) and exon 2 of the coding sequence breakpoints: AAGTACAACAGGATTTTTTT/TTTGATAACTTTTATTTCG. Breakpoints for E122: GCTGATATTTTCGAG/CGTTCCGTGTGACGTG and for E70: ATCTCCATATGCTCGTTTT/TTCCGTGTGACGTGAAAAGT.

All three deletions are lethal and were recombined with FRT80B (Xu and Rubin, 1993) and maintained balanced over *Tm6b*.

Cloning and Transgenic Flies

cDNAs of *fwe*^{ubi}, *fwe*$^{Lose\text{-}A}$, and *fwe*$^{Lose\text{-}B}$ as well as the *fwe*^{delC} sequence (see Figure S5) were fully sequenced and subcloned into the *pUASp* vector using KpnI (BamHI for *fwe*^{ubi}) and XbaI restriction sites. In order to generate N- and C-terminal HA-tagged forms, the respective cDNAs were amplified with primers containing the HA sequence and subcloned into KpnI and XbaI sites of *pUASp*. Primer sequences are available upon request. Multiple transgenic lines with insertion on different chromosomes were generated by Bestgene.

RNAi Lines

For *CG9233,* two independent transformants 19804 and 19805 were used that gave similar results (data shown for 19804). For *CG1084,* two independent transformants, 28294 and 40613, were used that gave similar results. For *CG4672,* transformant 8380 was used. For *CG6151* transformants 39596, 104993 (VDRC) and stock 27323 (Bloomington) were tested for rescue of WT loser cells and gave similar results. Data for 39596 are shown, which targets exon-3 and exon-4, common to all three *CG6151* isoforms. For *CG2198,* two independent transformants, 22944 and 22945, were used that gave similar results .For *CG3305* two independent transformants, 7308 and 7309 (data shown), gave similar results. All the data shown in Figure 2 were obtained from female larvae in order to minimize growth variability. For rescue of Eiger-induced cell death in the eye (Figure S4), we used transformants 45252 and 45253.

Quantifications

All error bars represent the standard error of the mean, except in Figure 7, where the standard deviation is shown.

ACCESSION NUMBERS

The data discussed in this publication have been deposited in NCBI's Gene Expression Omnibus and are accessible through GEO Series accession number GSE21230.

SUPPLEMENTAL INFORMATION

Supplemental Information includes seven figures, six videos, and Supplemental Experimental Procedures and can be found with this article online at doi:10.1016/j.devcel.2010.05.010.

ACKNOWLEDGMENTS

We thank K. Basler, S. Carroll, M.F. Ruiz, L. Sanchez, G. Morata, N. Baker, the Developmental Hybridoma Bank, and the Bloomington and Vienna VDRC stock centers for materials; Guadalupe Luengo and the Genomic Unit of CNIO; Fernando Roncal, Leonor Kremer, and Giovanna Roncador for help in antibody production; Diego Megías and María Montoya for help with confocal microscopy; Miguel Torres and Offer Gerlitz for critically reading the manuscript; Iñaki Ruiz-Trillo for discussions about the evolution of multicellularity, and the European Research Council, the Fundación Mutua Madrileña, the Fundación Caja Madrid, and the Comunidad of Madrid for support. The authors declare no competing interests.

Received: March 18, 2010
Revised: March 25, 2010
Accepted: April 8, 2010
Published: June 14, 2010

REFERENCES

Adachi-Yamada, T., and O'Connor, M.B. (2002). Morphogenetic apoptosis: a mechanism for correcting discontinuities in morphogen gradients. Dev. Biol. *251*, 74–90.

Adachi-Yamada, T., and O'Connor, M.B. (2004). Mechanisms for removal of developmentally abnormal cells: cell competition and morphogenetic apoptosis. J. Biochem. *136*, 13–17.

Adachi-Yamada, T., Fujimura-Kamada, K., Nishida, Y., and Matsumoto, K. (1999). Distortion of proximodistal information causes JNK-dependent apoptosis in Drosophila wing. Nature *400*, 166–169.

Brand, A.H., and Perrimon, N. (1993). Targeted gene expression as a means of altering cell fates and generating dominant phenotypes. Development *118*, 401–415.

Brumby, A.M., and Richardson, H.E. (2003). scribble mutants cooperate with oncogenic Ras or Notch to cause neoplastic overgrowth in Drosophila. EMBO J. *22*, 5769–5779.

Burke, R., and Basler, K. (1996). Dpp receptors are autonomously required for cell proliferation in the entire developing Drosophila wing. Development *122*, 2261–2269.

Celniker, S.E., Wheeler, D.A., Kronmiller, B., Carlson, J.W., Halpern, A., Patel, S., Adams, M., Champe, M., Dugan, S.P., Frise, E., et al. (2002). Finishing

a whole-genome shotgun: release 3 of the Drosophila melanogaster euchromatic genome sequence. Genome Biol. *3*, RESEARCH0079.

de la Cova, C., Abril, M., Bellosta, P., Gallant, P., and Johnston, L.A. (2004). *Drosophila* Myc regulates organ size by inducing cell competition. Cell *117*, 107–116.

Diaz, B., and Moreno, E. (2005). The competitive nature of cells. Exp. Cell Res. *306*, 317–322.

Dietzl, G., Chen, D., Schnorrer, F., Su, K.C., Barinova, Y., Fellner, M., Gasser, B., Kinsey, K., Oppel, S., Scheiblauer, S., et al. (2007). A genome-wide transgenic RNAi library for conditional gene inactivation in *Drosophila*. Nature *448*, 151–156.

Faivre-Sarrailh, C., Banerjee, S., Li, J., Hortsch, M., Laval, M., and Bhat, M.A. (2004). *Drosophila* contactin, a homolog of vertebrate contactin, is required for septate junction organization and paracellular barrier function. Development *131*, 4931–4942.

Gallant, P. (2005). Myc, cell competition and compensatory proliferation. Cancer Res. *65*, 6485–6487.

Grether, M.E., Abrams, J.M., Agapite, J., White, K., and Steller, H. (1995). The head involution defective gene of *Drosophila melanogaster* functions in programmed cell death. Genes Dev. *9*, 1694–1708.

Grewal, S.S., Li, L., Orian, A., Eisenman, R.N., and Edgar, B.A. (2005). Myc-dependent regulation of ribosomal RNA synthesis during *Drosophila* development. Nat. Cell Biol. *7*, 295–302.

Halder, G., Polaczyk, P., Kraus, M.E., Hudson, A., Kim, J., Laughon, A., and Carroll, S. (1998). The Vestigial and Scalloped proteins act together to directly regulate wing-specific gene expression in *Drosophila*. Genes Dev. *12*, 3900–3909.

Hay, B.A., Wolff, T., and Rubin, G.M. (1994). Expression of baculovirus P35 prevents cell death in *Drosophila*. Development *120*, 2121–2129.

Hay, B.A., Wassarman, D.A., and Rubin, G.M. (1995). *Drosophila* homologs of baculovirus inhibitor of apoptosis proteins function to block cell death. Cell *83*, 1253–1262.

Hoeppner, D.J., Hengartner, M.O., and Schnabel, R. (2001). Engulfment genes cooperate with ced-3 to promote cell death in Caenorhabditis elegans. Nature *412*, 202–206.

Hsiung, F., Ramirez-Weber, F.A., Iwaki, D.D., and Kornberg, T.B. (2005). Dependence of Drosophila wing imaginal disc cytonemes on Decapentaplegic. Nature *437*, 560–563.

Johnston, L.A., Prober, D.A., Edgar, B.A., Eisenman, R.N., and Gallant, P. (1999). *Drosophila* myc regulates cellular growth during development. Cell *98*, 779–790.

Lambertsson, A. (1998). The Minute genes in *Drosophila* and their molecular functions. Adv. Genet. *38*, 69–134.

Lee, T., Winter, C., Marticke, S.S., Lee, A., and Luo, L. (2000). Essential roles of *Drosophila* RhoA in the regulation of neuroblast proliferation and dendritic but not axonal morphogenesis. Neuron *25*, 307–316.

Li, W., and Baker, N.E. (2007). Engulfment is required for cell competition. Cell *129*, 1215–1225.

Marygold, S.J., Roote, J., Reuter, G., Lambertsson, A., Ashburner, M., Millburn, G.H., Harrison, P.M., Yu, Z., Kenmochi, N., Kaufman, T.C., et al. (2007). The ribosomal protein genes and Minute loci of *Drosophila melanogaster*. Genome Biol. *8*, R216.

Martín, F.A., and Morata, G. (2006). Compartments and the control of growth in the Drosophila wing imaginal disc. Development *133*, 4421–4426.

Milàn, M. (2002). Survival of the fittest. Cell competition in the *Drosophila* wing. EMBO Rep. *3*, 724–725.

Morata, G., and Ripoll, P. (1975). *Minutes*: mutants of *Drosophila* autonomously affecting cell division rate. Dev. Biol. *42*, 211–221.

Moreno, E. (2008). Is cell competition relevant to cancer? Nat. Rev. Cancer *8*, 141–147.

Moreno, E., and Basler, K. (2004). dMyc transforms cells into super-competitors. Cell *117*, 117–129.

Moreno, E., Basler, K., and Morata, G. (2002a). Cells compete for Decapentaplegic survival factor to prevent apoptosis in *Drosophila* wing development. Nature *416*, 755–759.

Moreno, E., Yan, M., and Basler, K. (2002b). Evolution of TNF signaling mechanisms: JNK-dependent apoptosis triggered by Eiger, the Drosophila homolog of the TNF superfamily. Curr. Biol. *12*, 1263–1268.

Orian, A., van Steensel, B., Delrow, J., Bussemaker, H.J., Li, L., Sawado, T., Williams, E., Loo, L.W., Cowley, S.M., Yost, C., et al. (2003). Genomic binding by the *Drosophila* Myc, Max, Mad/Mnt transcription factor network. Genes Dev. *17*, 1101–1114.

Rhiner, C., Díaz, B., Portela, M., Poyatos, J.F., Fernández-Ruiz, I., López-Gay, J.M., Gerlitz, O., and Moreno, E. (2009). Persistent competition among stem cells and their daughters in the *Drosophila* ovary germline niche. Development *136*, 995–1006.

Senoo-Matsuda, N., and Johnston, L.A. (2007). Soluble factors mediate competitive and cooperative interactions between cells expressing different levels of Drosophila Myc. Proc. Natl. Acad. Sci. USA *104*, 18543–18548.

Seeger, M.A., Haffley, L., and Kaufman, T.C. (1988). Characterization of amalgam: a member of the immunoglobulin superfamily from *Drosophila*. Cell *55*, 589–600.

Simpson, P. (1979). Parameters of cell competition in the compartments of the wing disc of *Drosophila*. Dev. Biol. *69*, 182–193.

Simpson, P., and Morata, G. (1981). Differential mitotic rates and patterns of growth in compartments in the *Drosophila* wing. Dev. Biol. *85*, 299–308.

Strigini, M., and Cohen, S.M. (2000). Wingless gradient formation in the *Drosophila* wing. Curr. Biol. *10*, 293–300.

Tanimoto, H., Itoh, S., ten Dijke, P., and Tabata, T. (2000). Hedgehog creates a gradient of DPP activity in *Drosophila* wing imaginal discs. Mol. Cell *5*, 59–71.

Xu, T., and Rubin, G.M. (1993). Analysis of genetic mosaics in developing and adult Drosophila tissues. Development *117*, 1223–1237.

Yao, C.K., Lin, Y.Q., Ly, C.V., Ohyama, T., Haueter, C.M., Moiseenkova-Bell, V.Y., Wensel, T.G., and Bellen, H.J. (2009). A synaptic vesicle-associated Ca2+ channel promotes endocytosis and couples exocytosis to endocytosis. Cell *138*, 947–960.

Ziv, O., Suissa, Y., Neuman, H., Dinur, T., Geuking, P., Rhiner, C., Portela, M., Lolo, F., Moreno, E., and Gerlitz, O. (2009). The co-regulator dNAB interacts with Brinker to eliminate cells with reduced Dpp signaling. Development *136*, 1137–1145.